Mode selection schemes for D2D enabled unmanned aerial vehicle-based wireless networks

Omri, Aymen; Hasna, Mazen O.; Shakir, Muhammad Zeeshan; Shaqfeh, Mohammed

Published in:
IET Communications

DOI:
10.1049/iet-com.2018.5834

Published: 25/06/2019

Document Version
Peer reviewed version

IET Journals
The Institution of Engineering and Technology

Mode Selection Schemes for D2D Enabled UAV-based Wireless Networks

ISSN 1751-8644
doi: 0000000000
www.ietdl.org

Aymen Omri[1]*, *Mazen O. Hasna*[2], *Muhammad Zeeshan Shakir*[3], *Mohammed Shaqfeh*[1]

[1] *Department of Electrical and Computer Engineering, Texas A&M University at Qatar.*
[2] *Electrical Engineering Department, Qatar University, Doha, Qatar*
[3] *School of Engineering and Computing, University of the West of Scotland, Paisley, Scotland-UK*
* *E-mail: aymen.omri@qatar.tamu.edu*

Abstract: In this paper, we present and evaluate the performance of two mode selection schemes for device to device (D2D) enabled UAV-based wireless networks. The proposed schemes are based on a threshold received signal strength (RSS) and an average threshold D2D distance to select the D2D mode. The focus of the two schemes is either to enhance the quality of the signal or the connectivity in case of emergency situations. To evaluate the performances of the schemes, we derive the corresponding expressions of the probability of using D2D mode and the average ergodic capacity. Numerical results show the advantage of the presented schemes in offloading traffic from aerial platforms and shed lights on the effect of environment on the performance of D2D enabled aerial networks.

1 Introduction

Network Flying Platforms (NFPs), such as drones and unmanned aerial vehicles (UAVs), have been proposed as promising solutions for future cellular networks [1–3]. In particular, NFPs can be used to enhance the wireless capacity and expand the coverage for temporary events, where there is a high density of users in a limited area, e.g., sports events and concert gatherings. Furthermore, NFPs can be deployed for unexpected scenarios, such as in emergency situations to support disaster relief activities and to enable communications when conventional terrestrial networks are either damaged or crowded. In addition, owing to their mobility, NFPs can be quickly and efficiently deployed to support cellular networks and enhance network quality-of-service (QoS) [2, 3].

For the mentioned scenarios, where there is no infrastructure or it is difficult to deploy one due to limited resources/support, direct device-to-device (D2D) communication helps in offloading traffic from NFPs, which will be helping all ground users in maintaining their links and in establishing the D2D links.

Considerable recent work have studied the use of D2D communications between wireless users over the licensed spectrum [4–8]. Different from NFP based communications, the D2D mode offers a direct transmission between users in physical proximity, without going through the NFPs in the network. However, when the users are far from each other, the NFP based aerial network may outperforms the D2D communication system. As a result, mode selection schemes for D2D enabled UAV-based wireless networks is very important and critical.

In the literature, various research work have investigated and evaluated the performances of D2D enabled UAV-based wireless networks in terms of link availability and sum throughput.

In [1], a drone-assisted multi-hop D2D communication scheme has been proposed to extend the network coverage over regions where it is difficult to deploy a terrestrial relay. In [2], the authors have analyzed the coverage of UAV-based wireless communications in the presence of D2D communication links. The advantage of alternative connectivity, between D2D transmission mode and drone-assisted communications, have been evaluated in [3], where the authors have shown an enhancement of 40 percent in the system performance in term of link availability and reliability. In [9], the UAV connected users and D2D receivers simultaneously operating in D2D underlaying UAV-assisted networks have been considered, where the authors have investigated the outage probability and derived its closed-form expression.

In [10], the authors have proposed an evaluated a low-complexity power control algorithm to improve the throughput of D2D communications underlaying UAV-assisted access systems. Another work has been presented in [11] to maximize the rate of a D2D pair for a DL UAV-aided wireless communication system, where the transmit power of the UAV and D2D users, the flying altitude and location of the UAV and ground terminalsâĂŹ allocated bandwidth have been jointly optimized. The corresponding simulation results have shown that the altitude of the UAV has an important impact on the system performance. In [12], a new spectrum sharing method for an aerial UAV and terrestrial D2D communications has been proposed and evaluated to maximize the sum throughput for a full-duplex UAV relaying systems with underlaid D2D communications. The partially overlapping channels (POCs) and game theory have been used in [13] to enhance the system performance of a combined UAV and D2D-based network in terms of good throughput and low signaling overhead in a dynamic environment.

All the above work have been focusing on evaluating the performance of D2D enabled aerial network without proposing mode selection mechanism, which is a very important technique for D2D-enabled aerial networks in general.

Different from D2D enabled aerial networks, the literature is rich with different mode selection schemes for D2D-enabled terrestrial wireless communication networks.

In [14], the author has investigated the performance of a mode selection scheme for D2D communication in heterogeneous cellular networks, where he has derived the outage probability expressions of the different communication modes. Then, he has proposed a mode selection scheme that is based on a lower bound expression of a D2D distance, which guarantees that the D2D outage probability is larger than a given QoS requirement. Finally, the outage probability metric has been used to evaluate the proposed mode selection scheme, when compared with the cellular mode. The lack of comparison between the performances of D2D and cellular modes presents a limitation of this work, i.e., the D2D mode can be used to offer the minimum required QoS in term of outage probability, with lower performance than that of the cellular mode.

Another work has been presented in [15], where the authors have used the stochastic geometry and the success probability metric to analyse and compare three proposed D2D mode selection methods in

the literature, namely the distance cut-off scheme [16], the link gain scheme [17], and the guard zone scheme [18]. The distance cut-off scheme is based on an optimum D2D mode selection threshold that minimizes the average transmit power of potential D2D user equipments (UEs) [16]. This optimum threshold has been defined as the D2D distance under which D2D communication should occur with a minimum average transmit power. For the link gain scheme, the D2D mode will be selected if the D2D link quality is at least as good as the cellular up-link (UL) quality [17]. The lack of consideration of the down-link (DL) quality presents a limitation on the performance of the proposed mode selection method in [17]. The third mode selection scheme that has been investigated in [15] is a guard-zone based mode selection mechanism [18]. This mode selection scheme is based on the comparison between the distance from the transmitter to the cellular BS and an optimal BSs guard zone radius that maximizes the total system throughput [18]. More specifically, if the UL distance is larger than the proposed optimal radius, then the cellular mode will be used. Otherwise, the D2D mode will be used, without interference impact on the active BSs. In this work, the maximizing problem of the total system throughput has been solved numerically to get the optimal guard zone radius, which presents a limitation in this work.

In [19], another mode selection method has been proposed, where the D2D mode can be used only if the D2D received signal strengths (RSSs) is larger than that of the cellular DL. Similar to the proposed mode selection in [17], the lack of consideration of both cellular links presents a limitation on the performance of the proposed mode selection scheme in [19]. Another mode selection scheme has been proposed in [20], where different from the work in [17] and [19], the proposed scheme is considering all the links between all the nodes in the network and is based on the comparison between the instantaneous D2D distance and a proposed average distance, where within this distance the D2D mode can be selected.

In the previous works [14–20], the altitude of the base stations is not considered to evaluate the distances, the RSSs and the SNRs between the different nodes in more realistic 3-D space, where a projection of the real distances between the nodes on 2-D space is used, which results in inaccurate values of the RSSs and the SNRs, especially for dense urban environments. In addition, most of the previous works have used the coverage probability or the success probability as performance analysis metric. However, these metrics are not the appropriate ones to evaluate the system performance in terms of link reliably and spectrum efficiency, where more efficient and accurate metrics can be used, such as the average ergodic capacity. Furthermore, the previous mode selection schemes are proposed for D2D-enabled terrestrial wireless communication networks and not for D2D enabled UAV-based wireless networks, where different air-to-ground channel model in 3-D space should be used [21].

In light of the aforementioned related work, our main contributions can be summarized as follows:

- We propose two mode selection schemes for D2D enabled UAV-based wireless networks. The proposed schemes are considering the D2D link as well as the cellular links. In addition, and different from the works in [20], the new schemes are based not only on an average threshold D2D distance, but also on a predefined threshold RSS. More details about the proposed mode selections are presented in Section 3.
- To describe the system model, and different from the work in [1–3], stochastic geometry is used in this paper to describe the different nodes' locations in the network. Moreover, and different from the previous works in [14–20], the system model is described in a more realistic 3-D space, with an accurate air-to-ground channel model [21]. Based on that, we derive the average ergodic capacity expressions for the D2D and cellular modes as well as for the proposed mode selection based transmission schemes, which are used to evaluate and investigate the advantage of the proposed mode selection schemes.

The rest of the paper is organized as follows. The system model is presented in Section 2. Section 3 introduces the proposed schemes.

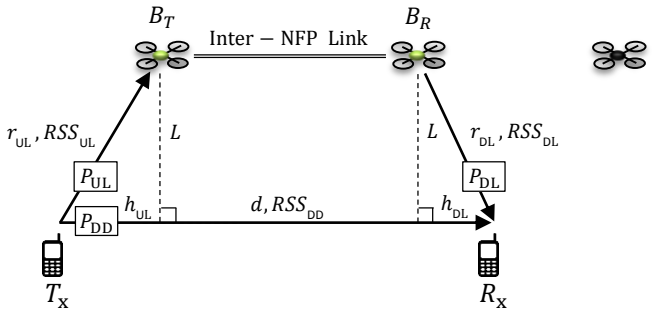

Fig. 1: The system model.

The performance analysis is detailed in Section 4, where the probability of using the D2D mode and the average ergodic capacity expressions are derived for both proposed schemes. Based on that, numerical results are presented in Section 5 to confirm the derived expressions and to investigate the advantages of the proposed schemes. Finally, conclusions are drawn in Section 6.

2 The System Model

2.1 Network Model

In this paper, a UAV-based wireless network is considered. The network consists of randomly located users, and a number of UAVs. The users are randomly located in the network, where the active transmitters are assumed to be located according to a Poisson point process (PPP) "Φ_T" with density λ_T. The position of the target receiver for each active transmitter is assumed to be randomly distributed according to a PPP "Φ_R" with density λ_R*. The locations of the UAVs are assumed to be distributed according to a Matérn hard-core process (MHCP) of Type II Φ_B, with the constraint of a minimum inter-distance δ between each two UAVs. Φ_B is based on a parent PPP Φ_P of density λ_P, where only the parent nodes that respect the inter-distance constraint are retained [22]. Accordingly, the density of Φ_B is expressed as [22]

$$\lambda_B = \frac{1 - \exp(-\pi\lambda_P\delta^2)}{\pi\delta^2}. \quad (1)$$

The simplified system model is presented in Fig. 1, and the main notations used throughout the paper are presented in Table 1.

2.2 Transmission Modes

Within the considered UAV-based wireless network system, a given transmitter T_x and a given receiver R_x can communicate using one of the following transmission modes:

2.2.1 Standard Transmission Mode: In this mode, T_x and R_x communicate with the corresponding nearest UAVs for the DL and the UL, where we assume that the UL and DL are decoupled, and that the UAVs have error free channel between them. Based on [21], the path-loss model for air-to-ground (AtG) communications is expressed as follows

$$PL_{AtG}(h, L) = 20\ \log_{10}\left(\frac{4\pi f_c}{C}\right) + 20\ \log_{10}(r) + P_{LOS}(h, L)\ \eta_{LOS} + [1 - P_{LOS}(h, L)]\ \eta_{NLOS}, \quad (2)$$

*We assume that the target receiver for a given active transmitter is located in the considered environment area of radius R. This is applicable, when the D2D users are close to each other, e.g., for same company users, or for internet of think (IoT) applications.

Table 1 Main notations used throughout the paper

Notation	Definition
λ_{T} [m^{-2}]	Density of the active transmitters.
λ_{R} [m^{-2}]	Density of the possible positions of a target receiver.
R [m]	Radius of the considered environment area.
λ_{B} [m^{-2}]	Density of the UAVs.
δ [m]	Minimum inter-distance between each two UAVs.
T_{x}	An active transmitter.
R_{x}	The target receiver for T_{x}.
f_c [Hz]	The carrier frequency.
C [m s^{-1}]	The speed of light.
r [m]	The distance between a user u and its nearest UAV.
h [m]	The horizontal distance between u and its nearest UAV.
L [m]	The altitude of the UAVs.
P_{LOS}	Probability of line of sight (LOS).
P_{NLOS}	Probability of non LOS (NLOS).
η_{LOS} [dB]	The LOS excessive loss.
η_{NLOS} [dB]	The NLOS excessive loss.
a and b	Constants environment parameters.
α	The path-loss exponent.
B_T	The nearest UAV to T_{x}.
B_R	The nearest UAV to R_{x}.
RSS_{X} [W]	RSS for the X link, X $\in \{DD, UL, DL\}$.
P_{X} [W]	Transmit power for the X link, X $\in \{DD, UL, DL\}$.
A_{X} [W]	The X link attenuation factor, X $\in \{DD, UL, DL\}$.
d [m]	The distance between T_{x} and R_{x}.
r_{UL} [m]	The distance between T_{x} and B_T.
r_{DL} [m]	The distance between B_R and R_{x}.
h_{UL} [m]	The horizontal distance between T_{x} and B_T.
h_{DL} [m]	The horizontal distance between B_R and R_{x}.
$\bar{d}_{\mathrm{th}}(L)$ [m]	The proposed average threshold D2D distance.
f	The PDF of r_{UL} and r_{DL}.
RSS_{th} [W]	A predefined D2D RSS threshold.
p	Probability of a user association to a UAV.
σ^2_{W} [W]	Additive white Gaussian noise (AWGN) power.

where, the LOS probability is expressed as follows

$$P_{\mathrm{LOS}}(h, L) = \frac{1}{1 + a \exp\Big(- b\Big[\arctan\Big(\frac{L}{h}\Big) - a\Big]\Big)}, \quad (3)$$

Based on that, the value of the air-to-ground signal attenuation can be presented as $A(h, L)\, r^{-2}$, where $A(h, L)$ is expressed as

$$A(h, L) = \Big(\frac{C}{4\pi f_c}\Big)^2 \, 10^{-\frac{P_{\mathrm{LOS}}(h,L)(\eta_{\mathrm{LOS}} - \eta_{\mathrm{NLOS}}) + \eta_{\mathrm{NLOS}}}{10}}, \quad (4)$$

and, $r = \sqrt{h^2 + L^2}$ is the distance between a given user and its serving nearest UAV.

2.2.2 D2D Transmission Mode: The D2D mode allows a direct transmission between users in proximity, where the UAVs role here is to facilitate and help establishing the D2D connection by exchanging the control and coordination signals. The path-loss model for D2D communications is given by

$$PL_{\mathrm{DD}}(d) = 20 \, \log_{10}\left(\frac{4\pi f_c}{C}\right) + 10\, \alpha \log_{10}(d). \quad (5)$$

Consequently, the D2D signal attenuation can be presented as $A_{\mathrm{DD}}\, d^{-\alpha}$, with $A_{\mathrm{DD}} = (C/[4\pi f_c])^2$.

3 Proposed Schemes Description

In this section, we propose two mode selection-based communication schemes for D2D-enabled aerial networks. The two proposed schemes are considering the RSSs of the D2D and aerial links, which are expressed as follows [19, 20]

$$RSS_{\mathrm{DD}} = P_{\mathrm{DD}}\, A_{\mathrm{DD}}\, d^{-\alpha}, \quad (6)$$

$$RSS_{\mathrm{UL}} = P_{\mathrm{UL}}\, A_{\mathrm{UL}}\, r_{\mathrm{UL}}^{-2}, \quad (7)$$

and,

$$RSS_{\mathrm{DL}} = P_{\mathrm{DL}}\, A_{\mathrm{DL}}\, r_{\mathrm{DL}}^{-2}, \quad (8)$$

respectively, where $A_{\mathrm{UL}} = A(h_{\mathrm{UL}}, L)$, and $A_{\mathrm{DL}} = A(h_{\mathrm{DL}}, L)$.
The proposed schemes are mainly based on a threshold D2D distance between T_{x} and R_{x}, where within this distance $RSS_{\mathrm{DD}} \geq \min(RSS_{\mathrm{UL}}, RSS_{\mathrm{DL}})$, and the D2D mode can be used to offer a better performance compared to the standard communication mode. Let $d_{\mathrm{th}}(L)$ be this distance that satisfies $RSS_{\mathrm{DD}} = \min(RSS_{\mathrm{UL}}, RSS_{\mathrm{DL}})$. Based on (6), $d_{\mathrm{th}}(L)$ can be expressed as

$$d_{\mathrm{th}}(L) = \left[\frac{P_{\mathrm{DD}}\, A_{\mathrm{DD}}}{\min(RSS_{\mathrm{UL}}, RSS_{\mathrm{DL}})}\right]^{\frac{1}{\alpha}}. \quad (9)$$

To evaluate the value of $d_{\mathrm{th}}(L)$, the levels of RSS_{UL}, and RSS_{DL} should be measured periodically, which increases the UL and DL signaling overhead. To prevent this problem, the proposed schemes are based on the average of $d_{\mathrm{th}}(L)$, $\bar{d}_{\mathrm{th}}(L)$, instead of its instantaneous value. In the following, we detail the derivation of $\bar{d}_{\mathrm{th}}(L)$.
By using the expressions of RSS_{UL} and RSS_{DL} in (7) and (8), the $d_{\mathrm{th}}(L)$ expression can be further represented as follows

$$d_{\mathrm{th}}(L) = \begin{cases} \left[\frac{P_{\mathrm{DD}}\, A_{\mathrm{DD}}}{P_{\mathrm{UL}}\, A_{\mathrm{UL}}}\right]^{\frac{1}{\alpha}} r_{\mathrm{UL}}^{\frac{2}{\alpha}}, & \text{if } r_{\mathrm{DL}} \leq \sqrt{\frac{P_{\mathrm{DL}}\, A_{\mathrm{DL}}}{P_{\mathrm{UL}}\, A_{\mathrm{UL}}}}\, r_{\mathrm{UL}} \\ \left[\frac{P_{\mathrm{DD}}\, A_{\mathrm{DD}}}{P_{\mathrm{DL}}\, A_{\mathrm{DL}}}\right]^{\frac{1}{\alpha}} r_{\mathrm{DL}}^{\frac{2}{\alpha}}, & \text{if } r_{\mathrm{UL}} \leq \sqrt{\frac{P_{\mathrm{UL}}\, A_{\mathrm{UL}}}{P_{\mathrm{DL}}\, A_{\mathrm{DL}}}}\, r_{\mathrm{DL}}. \end{cases} \quad (10)$$

To derive $\bar{d}_{\mathrm{th}}(L)$, the probability density function (PDF) expression of r_{UL} and r_{DL} is needed. Let $f(r)$ denotes this PDF, which is corresponding to the PDF of the distance between a given user and its nearest PDF. Based on [23], the exact expression of f is given by

$$f(r) = 2\lambda_{\mathrm{P}}\pi\sqrt{r^2 - L^2}\, \left[\frac{1 - \exp\Big(- \lambda_{\mathrm{P}}\Big[\pi\delta^2 - g\Big(\sqrt{r^2 - L^2}, \delta\Big)\Big]\Big)}{\lambda_{\mathrm{P}}\Big[\pi\delta^2 - g\Big(\sqrt{r^2 - L^2}, \delta\Big)\Big]}\right] \times \exp\left(\int_L^r 2\pi y \lambda_{\mathrm{P}} \left[\frac{1 - \exp\Big(- \lambda_{\mathrm{P}}\Big[\pi\delta^2 - g\Big(\sqrt{y^2 - L^2}, \delta\Big)\Big]\Big)}{\lambda_{\mathrm{P}}\Big[\pi\delta^2 - g\Big(\sqrt{y^2 - L^2}, \delta\Big)\Big]}\right] dy\right). \quad (11)$$

where,

$$g(x, \delta) = \begin{cases} 2\,\delta^2 \cos^{-1}\left(\frac{x}{2\,\delta}\right) - \frac{1}{2}\, x\, \sqrt{4\,\delta^2 - x^2}, & \text{if } 0 < x \leq 2\,\delta \\ 0, & \text{if } x > 2\,\delta. \end{cases} \quad (12)$$

The distance r in (11) is equal to r_{UL} for the UL case, and it is equal to r_{DL} for the DL case..
To get tractable analytical results for the proposed schemes, the following tight approximate PDF expression [24] is used instead of the expression in (11).

$$f(r) \approx 2\lambda_{\mathrm{B}}\pi r \, \exp\Big(- \lambda_{\mathrm{B}}\pi\Big[r^2 - L^2\Big]\Big). \quad (13)$$

Fig. 2 presents a comparison between the exact PDF expression in (11) and the approximate PDF expression in (13), while presenting

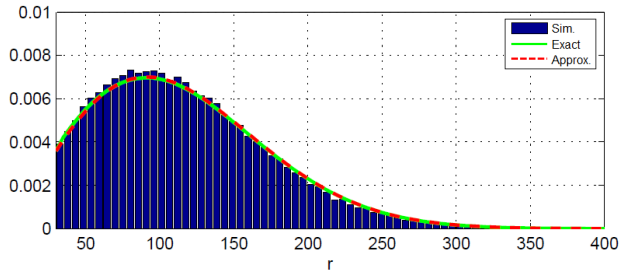

Fig. 2: PDF simulation of r as compared to the exact and approximate expressions in (11) and (13), respectively, with $\lambda_{\text{P}} = 2e-5/\text{m}^2$, $R = 500$ m, and $\delta = 100$ m.

the simulation results (histogram) of the distance r. The results in this figure confirm the accuracy of the approximate PDF expression, where an average error (compared to the exact PDF expression) of less than 2e$-$5 ($1.678e-05$) is observed.
Consequently, based on (13) and (10), the expression of $\bar{d}_{\text{th}}(L)$ is derived in Appendix 8.1 and is given by

$$\bar{d}_{\text{th}}(L) \approx 2\left[\frac{P_{\text{DD}}A_{\text{DD}}}{\pi\lambda_{\text{B}}P_{\text{UL}}\tilde{A}}\right]^{\frac{1}{\alpha}}\left[\exp\left(\lambda_{\text{B}}\pi L^2\right)\Gamma\left(\frac{\alpha+1}{\alpha},\lambda_{\text{B}}\pi L^2\right)\right.$$
$$\left.-\exp\left(2\lambda_{\text{B}}\pi L^2\right)\left[\frac{P_{\text{UL}}}{P_{\text{UL}}+P_{\text{DL}}}\right]^{\frac{\alpha+1}{\alpha}}\Gamma\left(\frac{\alpha+1}{\alpha},\left[\frac{P_{\text{UL}}+P_{\text{DL}}}{P_{\text{UL}}}\right]\lambda_{\text{B}}\pi L^2\right)\right]. \quad (14)$$

The approximation in (14) is due to using the approximate expression $\tilde{A}$ $(= A(1/[2\sqrt{\lambda_B}], L)$ of A_{UL} and A_{DL}, and the approximate expression of $f(r)$ in (13).

Accordingly, based on the average threshold D2D distance, we propose and evaluate the performance of the following transmission schemes.

3.1 Threshold D2D Distance based Scheme (TDDS)

In this scheme, T_{x} can transmit its message M to R_{x} by using either the D2D or standard transmission modes. The TDDS algorithm can be summarized as follows

Algorithm 1 : TDDS Algorithm

$M \neq \emptyset$
while $M \neq \emptyset$ **do**
  if $d \leq \bar{d}_{\text{th}}(L)$ **then**
    The D2D mode will be used.
  else
    if T_{x} is associated **then**
      The standard transmission mode will be used.
    else
      if $RSS_{\text{DD}} \geq RSS_{\text{th}}$ **then**
        The D2D mode will be used.
      Endif
    Endif
  Endif
  Updating d.
Endwhile

As shown in this Algorithm, the TDDS is based on RSS_{th}, $\bar{d}_{\text{th}}(L)$, and the D2D distance d, which we assume that are available for the corresponding nodes. Based on that, if $(d \leq \bar{d}_{\text{th}}(L))$, then the D2D mode will be used, where the users are assisted by the UAVs for D2D link establishment. Otherwise, and given that T_{x} is associated with a UAV, the standard transmission mode is used. If T_{x} is not associated, then the D2D mode is used if $RSS_{\text{DD}} \geq RSS_{\text{th}}$, which gives the possibility to the non associated users to directly communicate, while respecting a predefined RSS_{th}. Accordingly, a reduced signaling overhead can be observed as the proposed scheme is mainly based on predefined parameters $\bar{d}_{\text{th}}(L)$, RSS_{th}, and the actual distance d. In summary, the D2D mode for this scheme is used in two events: the first is when the distance d is less than or equal to $\bar{d}_{\text{th}}(L)$. The second event is when d is larger than $\bar{d}_{\text{th}}(L)$, T_{x} is not associated, and RSS_{DD} is larger or equal to RSS_{th}.

3.2 Received Signal Strength based Scheme (RSSS)

Similar to the TDDS algorithm, the mode selection in this scheme is based on $\bar{d}_{\text{th}}(L)$, RSS_{th}, and d. However, D2D mode is used only in the event in which RSS_{DD} is larger or equal to RSS_{th}. In the case of a large actual value of d, when $RSS_{\text{DD}} < RSS_{\text{th}}$ and $d > \bar{d}_{\text{th}}(L)$, the standard transmission mode may be used, as it outperforms the D2D mode in this case as shown in the following algorithm.

Algorithm 2 : RSSS Algorithm

$M \neq \emptyset$
while $M \neq \emptyset$ **do**
  if $RSS_{\text{DD}} \geq RSS_{\text{th}}$ **then**
    The D2D mode will be used.
  else
    if $d > \bar{d}_{\text{th}}(L)$ **then**
      if T_{x} is associated **then**
        The standard transmission mode will be used.
      Endif
    Endif
  Endif
  Updating d.
Endwhile

This scheme can be used for emergency communications, e.g., in the disaster cases, when a minimum small value of RSS_{th} is required to use the D2D mode.

4 Performance Analysis

In this section, we derive the probability of using D2D mode and the average ergodic capacity expressions for the two proposed schemes.

4.1 Probability of Using D2D Mode

Based on the proposed TDDS algorithm, the corresponding probability of using D2D mode can be written as follows

$$P_{\text{D2D}}^{\text{TDDS}} = Pr\left\{d \leq \bar{d}_{\text{th}}(L)\right\}$$
$$+ Pr\left\{(d > \bar{d}_{\text{th}}(L)) \cap (T_{\text{x}}\text{is not associated}) \cap (RSS_{\text{DD}} \geq RSS_{\text{th}})\right\}. \quad (15)$$

As presented in the system model, the users (including T_{x} and R_{x}) are randomly distributed according to PPPs. By considering the transmitter T_{x}, its target receiver R_{x} can be located at any point in the total considered area πR^2. Based on that, the expression of $P_{\text{D2D}}^{\text{TDDS}}$ can be derived as

$$P_{\text{D2D}}^{\text{TDDS}} = Pr\left\{d \leq \bar{d}_{\text{th}}(L)\right\} + \left(1-p\right)Pr\left\{\bar{d}_{\text{th}}(L) < d \leq \bar{r}_{\text{th}}\right\}$$
$$= \begin{cases} \frac{\bar{d}_{\text{th}}(L)^2}{R^2} + \frac{\left(\bar{r}_{\text{th}}^2 - \bar{d}_{\text{th}}(L)^2\right)(1-p)}{R^2}, & \text{if } (\bar{d}_{\text{th}}(L) \leq \bar{r}_{\text{th}} \leq R) \\ \frac{\bar{d}_{\text{th}}(L)^2}{R^2} + \left(1 - \frac{\bar{d}_{\text{th}}(L)^2}{R^2}\right)(1-p), & \text{elseif } (\bar{d}_{\text{th}}(L) \leq R < \bar{r}_{\text{th}}) \\ \frac{\bar{d}_{\text{th}}(L)^2}{R^2}, & \text{elseif } (\bar{r}_{\text{th}} \leq \bar{d}_{\text{th}}(L) \leq R) \\ 1, & \text{else,} \end{cases} \quad (16)$$

where, $\bar{r}_{\text{th}} = \sqrt{\frac{P_{\text{DD}} A_{\text{DD}}}{RSS_{\text{th}}}}$.
For the RSSS, and according to the second proposed algorithm, the probability of using D2D mode expression is given by

$$P_{D2D}^{\text{RSSS}} = Pr\Big\{RSS_{\text{DD}} \geq RSS_{\text{th}}\Big\} = Pr\left\{d \leq \bar{r}_{\text{th}}\right\}$$
$$= \begin{cases} \frac{\bar{r}_{\text{th}}^2}{R^2}, & \text{if } \left(RSS_{\text{th}} \geq \frac{P_{\text{DD}} A_{\text{DD}}}{R^2}\right) \\ 1, & \text{else.} \end{cases} \quad (17)$$

4.2 Average Ergodic Capacity

In this subsection, we derive first the average ergodic capacity expressions for D2D and standard modes, then we present the corresponding expressions of the proposed schemes.
For the D2D mode, the average ergodic capacity, denoted by $\bar{C}_{D2D}$, is derived in Appendix 8.2 and is expressed as

$$\bar{C}_{\text{D2D}} = \frac{1}{ln(2)} \sum_{n=1}^{N} \left\{ \frac{w_n P_{\text{DD}} A_{\text{DD}}}{\sigma_{\text{w}}^2 d^2 + x_n P_{\text{DD}} A_{\text{DD}}} \times \exp\left(- \frac{x_n \, \pi \lambda_{\text{T}} P_{\text{DD}} A_{\text{DD}} \log(Y_n + 1)}{\sigma_{\text{w}}^2} \right) \right\}, \quad (18)$$

where, $Y_n = \frac{R^2 \sigma_{\text{w}}^2}{x_n \, P_{\text{DD}} A_{\text{DD}}}$, x_n, and w_n are the n^{th} abscissa (root), and weight of the N^{th} order Laguerre polynomial, respectively.

The average ergodic capacity for the standard mode, denoted by $\bar{C}_{\text{Cel}}$, is derived in Appendix 8.3 and is expressed as

$$\bar{C}_{\text{Cel}} \approx \frac{1}{ln(2)} \sum_{n=1}^{N} \sum_{q=1}^{N} \frac{w_n w_q P_{\text{DL}} A_{\text{DL}}}{\sigma_{\text{w}}^2 (\frac{y_q}{\lambda_{\text{I}} \pi} + L_{\text{I}}^2) + P_{\text{DL}} \, \tilde{A} \, x_n} \times \exp\left(- x_n \, \frac{\pi \lambda_{\text{B}} P_{\text{DL}} \tilde{A} \log\left(\frac{1+Y_{n2}}{1+Y_{n1}}\right)}{\sigma_{\text{w}}^2} \right), \quad (19)$$

where, $Y_{n1} = (\frac{x_q}{\lambda_{\text{B}} \pi} + L_{\text{I}}^2) \frac{\sigma_{\text{w}}^2}{P_{\text{DL}} \, \tilde{A} \, x_n}$, and $Y_{n2} = \frac{(R^2 + L_{\text{I}}^2)\sigma_{\text{w}}^2}{P_{\text{DL}} \, \tilde{A} \, x_n}$.

Based on that, the expressions of the average ergodic capacity for the proposed schemes TDDS and RSSS are given by

$$\bar{C}_{\text{TDDS}} = \mathbf{I}(d, \bar{d}_{\text{th}}) \, \bar{C}_{\text{D2D}} + \mathbf{I}(\bar{d}_{\text{th}}, d) \left[p \, \bar{C}_{\text{Cel}} + (1-p) \, \mathbf{I}(d, \bar{r}_{\text{th}}) \, \bar{C}_{\text{D2D}} \right], \quad (20)$$

and

$$\bar{C}_{\text{RSSS}} = \mathbf{I}(d, \bar{r}_{\text{th}}) \, \bar{C}_{\text{D2D}} + \mathbf{I}(\bar{r}_{\text{th}}, d) \, \mathbf{I}(\bar{d}_{\text{th}}, d) \, p \, \bar{C}_{\text{Cel}}, \quad (21)$$

respectively, where $\mathbf{I}(x, y) = 1$, if $x \leq y$, and 0 otherwise.

5 Numerical results and Discussions

In this section, numerical results are presented to investigate the performance of the proposed schemes in terms of the probability of using D2D mode and the average ergodic capacity. Without loss of generality, the used simulation parameters are: $f_c = 2.5$ GHz, $R = 500$ m, $\lambda_{\text{B}} = 1e-4$ m^{-2}, $\delta = 100$ m, $\lambda_T = 1e-3$ m^{-2}, $\sigma_{\text{w}}^2 = -100$ dB, $P_{\text{DD}} = 300$ mW, $P_{\text{DL}} = P_{\text{UL}} = 0.5 \; P_{\text{DD}}$, $N = 30$, and $p = 0.8$. The different environment parameters are presented in the following table.

Fig. 3 presents the probability of using D2D mode vs. L for TDDS and RSSS algorithms, in a highrise urban environment, and with different values of RSS_{th}. As shown in this figure, for RSSS, P_{D2D} is invariable with the increased values of L, which is not the case for

Table 2 Environment Parameters [25]

	Suburban	Urban	Dense Urban	Highrise Urban
η_{LOS} $[dB]$	0.1	1	1.6	2.3
η_{NLOS} [dB]	21	20	23	34
(a, b)	(4.88, 0.43)	(9.61, 0.16)	(12.08, 0.11)	(27.23, 0.08)
α	2.7	2.9	3.1	3.5

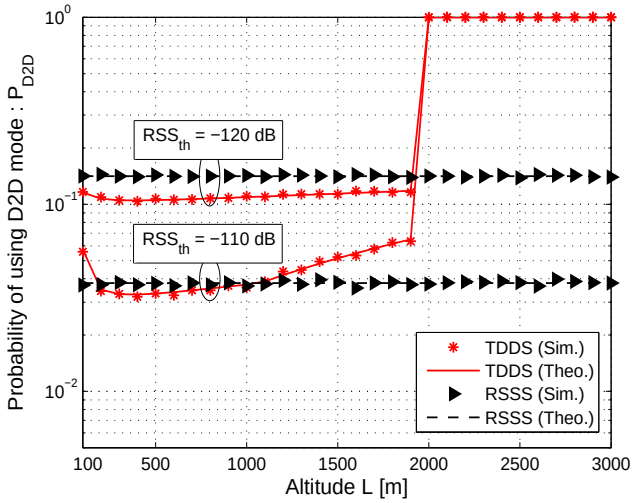

Fig. 3: Probability of using D2D mode vs. L, in a highrise urban environment, and with different values of RSS_{th}.

TDDS. This is due to the fact that the probability of using D2D mode within RSSS depends only on the values of RSS_{th}. However, for TDDS, this probability is not only inversely proportional to RSS_{th} but also depends on the height of the UAV. In fact, and based on Fig. 3, at low altitudes < 300 m, P_{D2D} decreases as L increases due to the increased LOS for both the UL and DL. However, if the height increases further, we notice that the D2D probability increases as the path-loss component for the standard communication mode starts to overcome the LOS component. This becomes more clear as the height increases further, beyond 2 km for the shown parameters where P_{D2D} becomes dominant and approaches 1.

In Fig. 4, the variation of P_{D2D} within TDDS vs. L is presented for different types of environments, with $RSS_{\text{th}} = -110$ dB. As

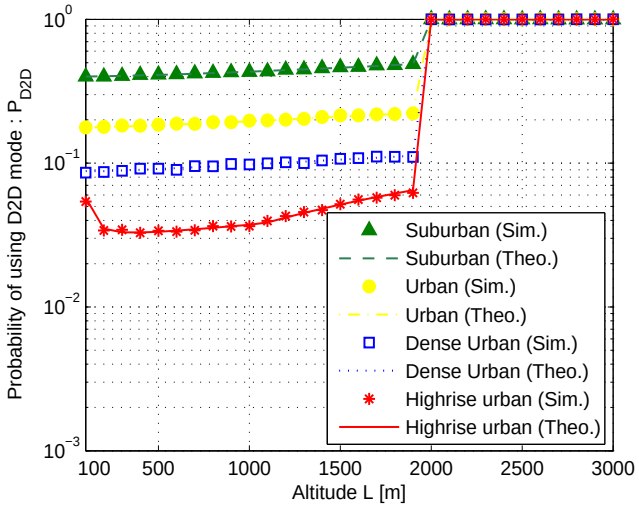

Fig. 4: Probability of using D2D mode within TDDS vs. L, in different environments, and with $RSS_{\text{th}} = -110$ dB.

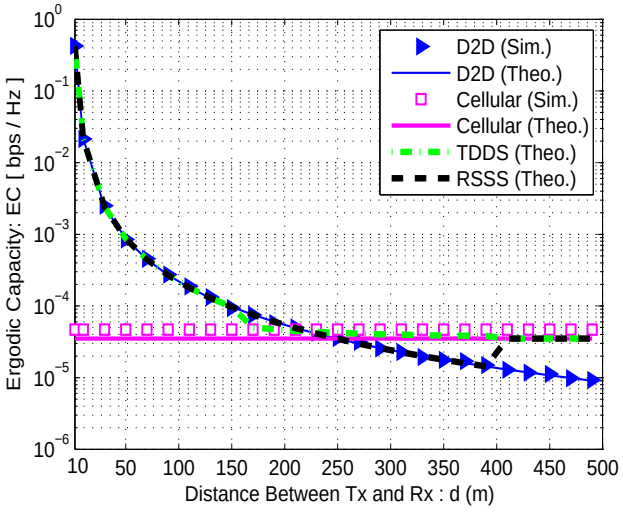

Fig. 5: Average ergodic capacity vs. d, in a dense urban environment for the different schemes, with $L = 100$ m, and $RSS_{\text{th}} = -120$ dB.

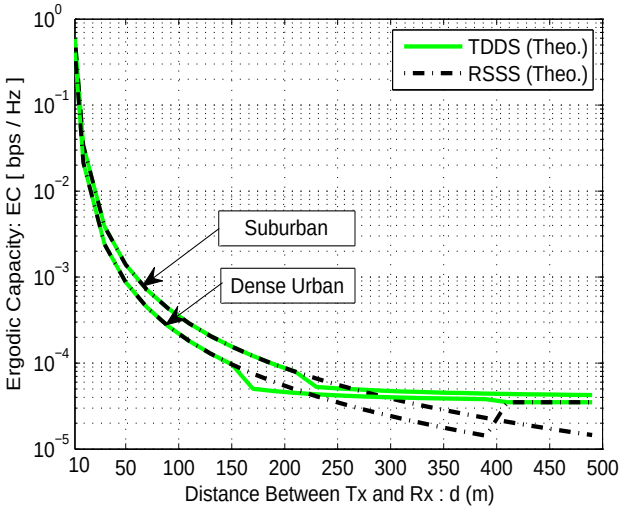

Fig. 6: Average ergodic capacity vs. d, in dense urban and suburban environments for the proposed schemes, with $L = 100$ m, and $RSS_{\text{th}} = -120$ dB.

shown in the figure, and for $L < 2$ km, P_{D2D} is higher for less dense environments. This is expected, as the LOS probability for D2D mode increases significantly with the decreased obstacles, when compared to the LOS probability for the standard mode. Consequently, an important enhancement of the D2D RSS can be observed, which results in an increase of the P_{D2D}. Again, at higher altitudes, D2D communication is dominant in all types of environments due to the severe path-loss component of the standard communication.

Fig. 5 presents the average ergodic capacity of the different transmission modes vs. d, in a dense urban environment. As shown in this figure, the new schemes TDDS and RSSS outperform the other schemes under-consideration, with better performance of TDDS. This is because, for short distance d, the proposed schemes select the D2D mode, which offers a better performance than standard mode, and for large D2D distance, they select the standard communication, which outperforms the D2D mode. Also, as the probability of using D2D mode is higher within RSSS compared to that of TDDS, the D2D mode for RSSS is selected even for large values of d when the standard mode is better, which is not the case for TDDS.

In Fig. 6, we present the average ergodic capacity of the proposed schemes vs. d, in a dense urban and a suburban environments. The simulation results confirm that the performance of both proposed schemes in the suburban environment is better than that in a dense urban environment, which is expected as the signal attenuation is larger in a dense urban environment than in a suburban environment. For this reason, and as shown in this figure, the RSSS is always using the D2D mode in the suburban environment, which is not the case in the dense urban environment.

Based on the simulation results, the proposed schemes offer the possibility to use the D2D mode for different scenarios with better performance when compared to the standard communications mode. Specifically, to improve the overall capacity of the users, and rather than optimizing the height of the UAVs, the D2D communication mode can be used by the associated users to the UAVs, not only to enhance the average users' capacity, but also to offload traffic from the aerial platforms and expand the network coverage.

6 Conclusion

Two mode selection schemes for D2D enabled UAV-based wireless networks are proposed and investigated in this paper. The two schemes are mainly based on a threshold RSS and an average threshold D2D distance between two given users to select the D2D mode. We have derived the corresponding expressions of the probability of using D2D mode and the averages ergodic capacity. Numerical results have been used to confirm the derived expressions, to evaluate the advantage of the proposed schemes, and to investigate the effect of environment on the performance of D2D enabled UAV-based wireless networks.

Acknowledgement

This paper was made possible by NPRP grant 8-1545-2-657 from the Qatar National Research Fund (a member of Qatar Foundation), and the sponsorship agreement in support of research and collaboration by Ooredoo, Doha, Qatar. The statements made herein are solely the responsibility of the authors.

7 References

1 Li, X., Guo, D., Yin, H., Wei, G.: 'Drone-Assisted Public Safety Wireless Broadband Network', *IEEE Wireless Commun and Networking Conf Workshops*, 2015,
2 Mozaffari, M., Saad, W., Bennis, M., Debbah, M.: 'Unmanned Aerial Vehicle with Underlaid Device-to-Device Communications: Performance and Tradeoffs', *IEEE Trans Wireless Commun*, 2016, **15**, (6), pp. 3949–3963
3 Orsino, A., et al.: 'Effects of Heterogeneous Mobility on D2D- and Drone-Assisted Mission-Critical MTC in 5G', *IEEE Commun Mag*, 2017, **55**, (2), pp. 79–87
4 Chou, H.J., Chang, R.Y.: 'Joint Mode Selection and Interference Management in Device-to-Device Communications Underlaid MIMO Cellular Networks', *IEEE Trans Wireless Commun*, 2017, **16**, (2), pp. 1120 – 1134
5 Hoang, T.D., Le, L.B., Le.Ngoc, T.: 'Joint Mode Selection and Resource Allocation for Relay-Based D2D Communications', *IEEE Commun Letters*, 2017, **21**, (2), pp. 398 – 401
6 Kazmi, S.M.A., et al.: 'Mode Selection and Resource Allocation in Device-to-Device Communications: A Matching Game Approach', *IEEE Trans Mobile Comput*, 2017, **16**, (11), pp. 3126 – 3141
7 Ma, R., Xia, N., Chen, H.H., Chiu, C.Y., Yang, C.S.: 'Mode Selection, Radio Resource Allocation, and Power Coordination in D2D Communications', *IEEE Wireless Commun*, 2017,
8 Wu, D., Wang, J., Hu, R.Q., Cai, Y., Zhou, L.: 'Energy-Efficient Resource Sharing for Mobile Device-to-Device Multimedia Commun.', *IEEE Trans on Vehicular Technology*, 2014, **63**, (5), pp. 2093 – 2103
9 Selim, M.M., Rihan, M., Yang, Y., Huang, L., Quan, Z., Ma, J.: 'On the Outage Probability and Power Control of D2D Underlaying NOMA UAV-Assisted Networks', *IEEE Access*, 2019,
10 Wang, H., Chen, J., Ding, G., Wang, S.: 'D2D Communications Underlaying UAV-Assisted Access Networks', *IEEE Access*, 2018, **6**, pp. 46244 – 46255
11 Huang, W., Yang, Z., Pan, C., Pei, L., Chen, M., Shikh.Bahaei, M., et al.: 'Joint Power, Altitude, Location and Bandwidth Optimization for UAV with Underlaid D2D Communications', *IEEE Wireless Commun Letters*, 2018,
12 Wang, H., Wang, J., Ding, G., Chen, J., Li, Y., Han, Z.: 'Spectrum Sharing Planning for Full-Duplex UAV Relaying Systems With Underlaid D2D Communications', *IEEE Journal on Selected Areas in Commun*, 2018, **36**, (9), pp. 1986 – 1999

13 Tang, F., Fadlullah, Z.M., Kato, N., Ono, F., Miura, R.: 'AC-POCA: Anti-coordination Game Based Partially Overlapping Channels Assignment in Combined UAV and D2D-Based Networks', *IEEE Transactions on Vehicular Technology*, 2018, **67**, (2), pp. 1672–1683

14 Xu, Y. 'A Mode Selection Scheme for D2D Communication in Heterogeneous Cellular Networks'. In: Proc. IEEE Global Commun. Conf. (GlobeCom). (, 2015. pp. 1–6

15 Marshall, D., Durrani, S., Guo, J., Yang, N. 'Performance comparison of device-to-device mode selection schemes'. In: Proc. IEEE Int. Symposium on Personal, Indoor, and Mobile Radio Commun. (PIMRC). (, 2015. pp. 1536–1541

16 Lin, X., Andrews, J.G., Ghosh, A.: 'Spectrum Sharing for Device-to-Device Communication in Cellular Networks', *IEEE Trans on Wireless Commun*, 2014, **13**, (12), pp. 6727–6740

17 ElSawy, H., Hossain, E., Alouini, M.S.: 'Analytical Modeling of Mode Selection and Power Control for Underlay D2D Communication in Cellular Networks', *IEEE Trans on Commun*, 2014, **62**, (11), pp. 4147–4161

18 Ye, J., Zhang, Y.J. 'A guard zone based scalable mode selection scheme in D2D underlaid cellular networks'. In: 2015 IEEE Int.Conf. on Commun. (ICC). (, 2015. pp. 2110–2116

19 Xu, X., Zhang, Y., Sun, Z., Hong, Y., Tao, X.: 'Analytical Modeling of Mode Selection for Moving D2D-Enabled Cellular Networks', *IEEE Commun Letters*, 2016, **20**, (6), pp. 1203 – 1206

20 Omri, A., Hasna, M.O.: 'A Distance Based Mode Selection Scheme for D2D Enabled Networks with Mobility', *IEEE Trans Wireless Commun*, 2018,

21 Yaliniz, R., Keyi, A., Yanikomeroglu, H.: 'Efficient 3-D Placement of an Aerial Base Station in Next Generation Cellular Networks', *IEEE International Conf on Commun (ICC)*, 2016,

22 Haenggi, M.: 'Mean Interference in Hard-Core Wireless Networks', *IEEE Commun Letters*, 2011, **15**, (8), pp. 792 – 794

23 Al.Hourani, A., Evans, R.J., Kandeepan, S.: 'Nearest Neighbor Distance Distribution in Hard-Core Point Processes', *IEEE Commun Letters*, 2016, **20**, (9), pp. 1872 – 1875

24 Omri, A., Hasna, M.O.: 'Modelling and Performance Analysis of 3-D Heterogeneous Networks with Interference Management', *IEEE Commun Letters*, 2017,

25 Al.Hourani, A., Kandeepan, S., Jamalipour, A.: 'Modeling air-to-ground path loss for low altitude platforms in urban environments', *IEEE Global Commun Conf*, 2014,

26 Gradshteyn, I.S., Ryzhik, I.M.: 'Table of Integrals, Series, and Products', *Elsevier Inc*, 2007,

27 Hamdi, K.A.: 'Capacity of MRC on Correlated Rician Fading Channels', *IEEE Trans Commun*, 2008, **56**, (5), pp. 708–711

28 Chiu, S.N., Stoyan, D., Kendall, W.S., Mecke, J.: 'Stochastic Geometry and its Applications', *John Wiley & Sons, Ltd*, 2013,

8 Appendices

8.1 Derivation of $\bar{d}_{th}(L)$

Based on (10), the expression of $\bar{d}_{\text{th}}(L)$ can be written as

$$\bar{d}_{\text{th}}(L) = \int_L^\infty \int_L^{\sqrt{\frac{P_{\text{DL}}\,A_{\text{DL}}}{P_{\text{UL}}\,A_{\text{UL}}}}r_{\text{UL}}} \left[\frac{P_{\text{DD}}\,A_{\text{DD}}}{P_{\text{UL}}\,A_{\text{UL}}}\right]^{\frac{1}{\alpha}} r_{\text{UL}}^{\frac{2}{\alpha}}\, f(r_{\text{UL}})\, f(r_{\text{DL}})\, dr_{\text{DL}}\, dr_{\text{UL}}$$
$$+ \int_L^\infty \int_L^{\sqrt{\frac{P_{\text{UL}}\,A_{\text{UL}}}{P_{\text{DL}}\,A_{\text{DL}}}}r_{\text{DL}}} \left[\frac{P_{\text{DD}}\,A_{\text{DD}}}{P_{\text{DL}}\,A_{\text{DL}}}\right]^{\frac{1}{\alpha}} r_{\text{DL}}^{\frac{2}{\alpha}}\, f(r_{\text{UL}})\, f(r_{\text{DL}})\, dr_{\text{UL}}\, dr_{\text{DL}}. \tag{22}$$

A tight approximation of the expressions of A_{UL} and A_{DL}, denoted by $\bar{A}$, can be used by substituting h with its mean value, $\bar{h} = \frac{1}{2\sqrt{\lambda_{\text{B}}}}$, in (4). Based on that, and by using the expressions of f in (13), the integration with respect to r_{DL}, in the first part, I_1, of the integrations in (22), is evaluated as follows

$$I_1 = \int_L^\infty \int_L^{\sqrt{\frac{P_{\text{DL}}\,A_{\text{DL}}}{P_{\text{UL}}\,A_{\text{UL}}}}r_{\text{UL}}} \left[\frac{P_{\text{DD}}\,A_{\text{DD}}}{P_{\text{UL}}\,A_{\text{UL}}}\right]^{\frac{1}{\alpha}} r_{\text{UL}}^{\frac{2}{\alpha}}\, f(r_{\text{UL}})\, f(r_{\text{DL}})\, dr_{\text{DL}}\, dr_{\text{UL}}$$
$$\approx \left[\frac{P_{\text{DD}}\,A_{\text{DD}}}{P_{\text{UL}}\,\bar{A}}\right]^{\frac{1}{\alpha}} \int_L^\infty \left[1 - \exp\left(-\lambda_{\text{B}}\pi\left[\frac{P_{\text{DL}}}{P_{\text{UL}}}\, r_{\text{UL}}^2 - L^2\right]\right)\right]$$
$$\times \left[2\lambda_{\text{B}}\,\pi\, r_{\text{UL}}^{1+\frac{2}{\alpha}}\, \exp\left(-\lambda_{\text{B}}\,\pi\left[r_{\text{UL}}^2 - L^2\right]\right)\right] dr_{\text{UL}} \tag{23}$$

By using the change in variables: $x = \lambda_{\text{B}}\pi r_{\text{UL}}^2$, and integration by parts [26, Eq. (3.381.3)], the integration in (23) is evaluated, which yields

$$I_1 \approx \left[\frac{P_{\text{DD}}\,A_{\text{DD}}}{\pi\lambda_{\text{B}}\,P_{\text{UL}}\,\bar{A}}\right]^{\frac{1}{\alpha}} \exp\left(2\lambda_{\text{B}}\pi L^2\right)\left[\exp\left(-\lambda_{\text{B}}\pi L^2\right)\Gamma\left(\frac{\alpha+1}{\alpha}, \lambda_{\text{B}}\pi L^2\right)\right.$$
$$\left. - \left[\frac{P_{\text{UL}}}{P_{\text{UL}}+P_{\text{DL}}}\right]^{\frac{\alpha+1}{\alpha}} \Gamma\left(\frac{\alpha+1}{\alpha}, \left[\frac{P_{\text{UL}}+P_{\text{DL}}}{P_{\text{UL}}}\right]\lambda_{\text{B}}\pi L^2\right)\right]. \tag{24}$$

Since the PDF expression of r_{UL} is the same as that of r_{DL}, the second part of the integrations in (22) is expressed as in (24). Based on that, the final expression of $\bar{d}_{\text{th}}(L)$ is given by (14), which completes the proof.

8.2 Derivation of $\bar{C}_{D2D}$

$\bar{C}_{\text{D2D}}$ expression is derived by using the following theorem [27]:

$$\mathbf{E}\Big[\ln\Big(1+\frac{S_{\text{DD}}}{I_{\text{DD}}+\sigma_{\text{w}}^2}\Big)\Big] = \int_0^\infty \left(\frac{1-\mathbf{L}_{S_{\text{DD}}}\left(\frac{x}{\sigma_{\text{w}}^2}\right)}{x}\right)\mathbf{L}_{I_{\text{DD}}}\left(\frac{x}{\sigma_{\text{w}}^2}\right) e^{-x}\, dx, \tag{25}$$

where, $\mathbf{L}_{S_{\text{DD}}}$ ($\mathbf{L}_{I_{\text{DD}}}$) is the Laplace transform of the non-negative random variable S_{DD} (I_{DD}). In this case, $S_{\text{DD}} = P_{\text{DD}}\, H_{\text{DD}}\, A_{\text{DD}}\, d^{-2}$, H_{DD} is the D2D channel gain, and I_{DD} is the total received interference at R_{x}. By using the exponential PDF expression of H_{DD}, $\mathbf{L}_{S_{\text{DD}}}\left(\frac{x}{\sigma_{\text{w}}^2}\right)$ is derived as follows

$$\mathbf{L}_{S_{\text{DD}}}\left(\frac{x}{\sigma_{\text{w}}^2}\right) = \mathbf{E}\left[\exp\left(\frac{-x\,S_{\text{DD}}}{\sigma_{\text{w}}^2}\right)\right]$$
$$= \int_0^\infty \exp\left(-H_{\text{DD}}\left(1+\frac{x\,P_{\text{DD}}\,A_{\text{DD}}\,d^{-2}}{\sigma_{\text{w}}^2}\right)\right) dH_{\text{DD}}$$
$$= \frac{\sigma_{\text{w}}^2}{\sigma_{\text{w}}^2 + x\,P_{\text{DD}}\,A_{\text{DD}}\,d^{-2}}. \tag{26}$$

According to the independence of the channel gain between the transmitter $T_{\text{i}} \in \Phi_{\text{T}}$ and R_{x}, denoted by $(H_{T_{\text{i}},R_{\text{x}}})$, $\mathbf{L}_{I_{\text{DD}}}(s)$ can be represented as

$$\mathbf{L}_{I_{\text{DD}}}[s] = \mathbf{E}_{\{\Phi_{\text{T}},H_{T_{\text{i}},R_{\text{x}}}\}}\left[\exp\left(-s\sum_{T_{\text{i}}\in\Phi_{\text{T}}} P_{\text{DD}}H_{T_{\text{i}},R_{\text{x}}}A_{\text{DD}}l_i^{-2}\right)\right]$$
$$= \mathbf{E}_{\Phi_{\text{T}}}\left[\prod_{T_{\text{i}}\in\Phi_{\text{T}}} \mathbf{E}_{\{H_{T_{\text{i}},R_{\text{x}}}\}}\left[\exp\left(-sP_{\text{DD}}H_{T_{\text{i}},R_{\text{x}}}A_{\text{DD}}l_i^{-2}\right)\right]\right], \tag{27}$$

where, l_i denotes the distance between T_{i} and R_{x}. Now, using the probability generating functional [28], and the PDF expressions of $H_{T_{\text{i}},R_{\text{x}}}$, $\mathbf{L}_{I_{\text{DD}}}[s]$ can be expressed as

$$\mathbf{L}_{I_{\text{DD}}}[s] = \exp\left(-2\pi\lambda_{\text{B}}\int_0^R \left(1-\frac{1}{1+sP_{\text{DD}}A_{\text{DD}}l^{-2}}\right) l\, dl\right). \tag{28}$$

By using the change in variables: $y = (\frac{x}{\sigma_{\text{w}}^2}\, P_{\text{DD}}A_{\text{DD}})^{-1} l^2$, and by letting $s = (\frac{x}{\sigma_{\text{w}}^2})$, (28) is rewritten as

$$\mathbf{L}_{I_{\text{DD}}}\left(\frac{x}{\sigma_{\text{w}}^2}\right) = \exp\left(-\frac{\pi\,\lambda_{\text{B}}\,P_{\text{DD}}\,A_{\text{DD}}\,x}{\sigma_{\text{w}}^2}\int_0^Y \frac{1}{1+y}\, dy\right), \tag{29}$$

where, $Y = \frac{R^2\sigma_{\text{w}}^2}{x\,P_{\text{DD}}\,A_{\text{DD}}}$.

Finally, by substituting (26) and (29) in (25), $\bar{C}_{\text{D2D}}$ is expressed as follows

$$\bar{C}_{\text{D2D}} = \frac{1}{ln(2)}\int_0^\infty \frac{P_{\text{DD}}A_{\text{DD}}}{\sigma_{\text{w}}^2 d^2 + xP_{\text{DD}}A_{\text{DD}}}$$
$$\times \exp\left(-x\,\frac{\sigma_{\text{w}}^2 + \pi\lambda_{\text{B}}P_{\text{DD}}A_{\text{DD}}\log(Y+1)}{\sigma_{\text{w}}^2}\right) dx. \tag{30}$$

Finally, based on Laguerre theorem, (30) is expressed as in (18).

8.3 Derivation of $\bar{C}_{Cel}$

Based on (25), $\bar{C}_{\text{Cel}}$ can be written as follows

$$\bar{C}_{\text{Cel}} \approx \int_0^{\infty} \int_L^{\infty} f(r_{\text{DL}}) \left(\frac{1 - \mathbf{L}_{S_{\text{DL}}} \left(\frac{x}{\sigma_{\text{w}}^2} \right)}{x} \right) \mathbf{L}_{I_{\text{DL}}} \left(\frac{x}{\sigma_{\text{w}}^2} \right) \exp(-x)\, dr\, dx, \tag{31}$$

where, $S_{\text{DL}} = P_{\text{DL}}\, H_{\text{DL}}\, A_{\text{DL}}\, r_{\text{DL}}^{-2}$, and H_{DL} is the DL channel gain. By analogy with the derivation of (26), $\mathbf{L}_{S_{\text{DL}}} \left(\frac{x}{\sigma_{\text{w}}^2} \right)$ is expressed as

$$\mathbf{L}_{S_{\text{DL}}} \left(\frac{x}{\sigma_{\text{w}}^2} \right) = \frac{\sigma_{\text{w}}^2}{\sigma_{\text{w}}^2 + x\, P_{\text{DL}}\, A_{\text{DL}}\, r_{\text{DL}}^{-2}}. \tag{32}$$

Based on the independence of the channel gain between the BS j and R_{x}, denoted by $H_{\text{B}_{\text{j}},R_{\text{x}}}$, $\mathbf{L}_{I_{\text{DL}}}(s)$ can be represented as

$$\begin{aligned} \mathbf{L}_{I_{\text{DL}}}[s] &= \mathbf{E}_{\{\Phi_{\text{l}}, H_{\text{B}_{\text{j}},R_{\text{x}}}\}} \left[\exp\left(- s \sum_{\text{B}_{\text{j}} \in \Phi_{\text{l}} \setminus \{\text{B}_{\text{R}}\}} P_{\text{DL}} H_{\text{B}_{\text{j}},R_{\text{x}}} A_{\text{DL}} d_j^{-2} \right) \right] \\ &= \mathbf{E}_{\Phi_{\text{l}}} \left[\prod_{\text{B}_{\text{j}} \in \Phi_{\text{l}} \setminus \{\text{B}_{\text{R}}\}} \mathbf{E}_{\{H_{\text{B}_{\text{j}},R_{\text{x}}}\}} \left[\exp\left(- s P_{\text{DL}} H_{\text{B}_{\text{j}},R_{\text{x}}} A d_j^{-2} \right) \right] \right], \end{aligned} \tag{33}$$

where, d_j denotes the distance between B_{j} and R_{x}. Using the probability generating functional [28] and the PDF expressions of $H_{\text{B}_{\text{j}},R_{\text{x}}}$, $\mathbf{L}_{I_{\text{DL}}}[s]$ can be expressed as

$$\mathbf{L}_{I_{\text{DL}}}[s] = \exp\left(- 2\pi\lambda_{\text{B}} \int_{r_{\text{DL}}}^{\sqrt{R^2+L^2}} \left(1 - \frac{1}{1 + s P_{\text{DL}} A_{\text{DL}} l^{-2}} \right) l\, dl \right). \tag{34}$$

Now, using the change in variables: $y = \left(\frac{x}{\sigma_{\text{w}}^2}\, P_{\text{DL}} A_{\text{DL}} \right)^{-1} l^2$, and by letting $s = \left(\frac{x}{\sigma_{\text{w}}^2} \right)$, (28) is rewritten as

$$\mathbf{L}_{I_{\text{DL}}} \left(\frac{x}{\sigma_{\text{w}}^2} \right) = \exp\left(- \frac{\pi\, \lambda_{\text{B}}\, P_{\text{DL}}\, A_{\text{DL}}\, x}{\sigma_{\text{w}}^2} \int_{Z_1}^{Z_2} \frac{1}{1+y}\, dy \right), \tag{35}$$

where, $Z_1 = \frac{r_{\text{DL}}^2 \sigma_{\text{w}}^2}{x\, P_{\text{DL}}\, A_{\text{DL}}}$, and $Z_2 = \frac{(R^2+L^2)\sigma_{\text{w}}^2}{x\, P_{\text{DL}}\, A_{\text{DL}}}$.

By substituting (32) and (35) in (31), $\bar{C}_{\text{Cel}}$ is expressed as follows

$$\begin{aligned} \bar{C}_{\text{Cel}} \approx\ & \frac{1}{ln(2)} \int_0^{\infty} \int_{L_1}^{\infty} 2\lambda_{\text{B}} \pi r_{\text{DL}}\, \exp\left(-\lambda_{\text{B}} \pi \left[r_{\text{DL}}^2 - L^2 \right] \right) \\ & \times \frac{P_{\text{DL}} A_{\text{DL}}}{\sigma_{\text{w}}^2 r_{\text{DL}}^2 + x P_{\text{DL}} A_{\text{DL}}} \exp\left(- x\, \frac{\sigma_{\text{w}}^2 + \pi\lambda_{\text{B}} P_{\text{DL}} A_{\text{DL}} \log\left(\frac{1+Y_2}{1+Y_1} \right)}{\sigma_{\text{w}}^2} \right) dr dx, \end{aligned} \tag{36}$$

where, $Y_1 = \left(\frac{x}{\lambda_{\text{B}} \pi} + L^2 \right) \frac{\sigma_{\text{w}}^2}{P_{\text{DL}}\, \tilde{A}\, x}$, and $Y_2 = \frac{(R^2+L^2)\sigma_{\text{w}}^2}{P_{\text{DL}}\, \tilde{A}\, x}$.

Finally, by using the Laguerre theorem, (36) is expressed as in (19).